Hindawi
Mathematical Problems in Engineering
Volume 2019, Article ID 8129564, 14 pages
https://doi.org/10.1155/2019/8129564

Research Article

Mixed Convection Magnetohydrodynamics Flow of a Nanofluid with Heat Transfer: A Numerical Study

Abdul Quayam Khan and Amer Rasheed

Department of Mathematics, School of Science and Engineering, Lahore University of Management Sciences, Opposite Sector U, DHA, Lahore Cantt. 54792, Pakistan

Correspondence should be addressed to Amer Rasheed; amer.rasheed@lums.edu.pk

Received 10 August 2018; Revised 6 January 2019; Accepted 15 January 2019; Published 21 January 2019

Academic Editor: Gilberto Espinosa-Paredes

In this paper we have studied the magnetohydrodynamic (MHD) mixed convection Maxwell flow of an incompressible nanofluid with magnetic field and heat transfer over a moving plate aligned horizontally. Thermal radiation has also been applied in order to investigate its effects on velocity and temperature variations in the fluid. The Caputo time derivative has been employed to derive the mathematical model. A numerical solution has been obtained using finite difference discretization along with $L1$-algorithm. Fractional and other pertinent physical fluid parameters like magnetic field parameter, thermal radiation, effect on velocity, and temperature distribution are analyzed and demonstrated through graphs.

1. Introduction

Heat transfer and viscoelastic fluid flow gain much attention because it has widespread applications in several fields of science and engineering. Maxwell fluid model, also known as viscoelastic rate type fluid model, was introduced by James Clerk Maxwell [1] in his research article on the dynamical theory of gases. The Maxwell model has advantage of being expressed as a differential model in a basic form. This permits comparison between results of different methods. Much work has been done by many researchers in Maxwell fluids. Hayat et al. [2] studied Maxwell fluid flow of heterogeneous and homogeneous processes in the stagnation region over a stretched surface and analyzed the behavior of a flow with several set of physical parameters. Zhi Cao et al. [3] have investigated the effect of magnetic field on a fractional Maxwell nanofluid over a moving plate and also discussed the temperature variations due to nanoparticles present in the base fluid using $L1$ scheme along with finite difference approximations. Liu and Guo [4] studied MHD flow of Maxwell liquid with slip conditions pursued by a moving plate. Mashud et al. [5] examined a Maxwell fluid of unsteady flow with boundary layer approximation. Madhu et al. [6] analyzed MHD flow of a Maxwell nanofluid with thermal radiation and stretching surface and also discussed flow behavior of a Maxwell nanofluid using different values of physical parameters. Vieru and Rauf [7] investigated Maxwell flow in a channel with slip conditions and found exact as well as approximate solution of a model and discussed slip coefficient effects on velocity. Hsiao [8] studied the Maxwell fluid model of a thermal extrusion energy conversation problem and solved it by using numerical techniques. Hayat et al. [9] investigated the rotating flow of Maxwell liquid in three-dimensional nanofluid wherein the fluid was moving with the help of an exponentially stretching sheet and solved the problem by Homotopy Analysis Method. Ramesh et al. [10] investigated the Maxwell fluid model of stagnation point flow on a stretching sheet and found an approximate solution of the model by using Runge Kutta Fehlberg Method. Mukopadhyay [11] investigated the Maxwell fluid model of MHD over stretching sheet using temperature on the surface and numerically solved the problem by Shooting Method and also analyzed fluid behavior with different physical parameters.

The enhancement of thermal conductivity with base fluid and heat transfer improvement of fluids is an important research topic due to its tremendous applications in industry and sciences. Heat transfer fluids have a new category

known as nanofluids and were first suggested by Choi and Eastman [15] and refer to a liquid which is heated by diverged nanoparticles into a base fluid. Nanofluid is a fluid having nanometer (small diameters of nanoscale) size elements, known as nanoparticles. Nanoparticles can be metallic, for example, (Fe, Al, Ag, Au, Cu), or nonmetallic, for example, $(Al_2O_3, Fe_2O_3, CuO, TiO_2, SiO_2)$, and could also be carbon nanotubes, for example, $(CNT, MWCNT, SWCNT)$. Nanofluids enhance thermal properties compared to the base fluids and this fact makes nanofluids an alternative working fluids. More precisely, nanoparticles enhance thermal conductivity, viscosity, and density but decrease specific heat capacity. Prasannakumara et al. [16] studied radiative heat transfer of nanofluids using magnetic field over a plate. They noticed that the Nusselt number and Sherwood number are increased for nonlinear stretching sheet. Kumar et al. [17] investigated the Marangoni effects on nanofluid in the presence of heat. Sheikholeslami and Shehzad [18] studied heat transfer of nonequilibrium model for nanofluid with magnetic field and porous medium. Turkyilmazoglu and Pop [19] studied heat and mass transfer of free convection flow of nanofluid containing Al_2O_3, Cu, Ag, CuO, and TiO_2 as nanoparticles. They conclude that the fluid having particles of kind TiO_2 have low heat transfer and with Cu have maximum heat transfer. Recently various researchers studied heat transfer of nanofluids; see, for example, [20–24].

Radiation for heat transfer is important because of its wide applications in nuclear power generation, reactor cooling, and combustion applications. The best possible comprehension of instrument of solar radiation has real significance in the plan of advance energy conversation system performed at high temperature. Some examples of these are space vehicle reentry, astrophysical flows, fossil fuel, solar power technology, and combustion energy. Such impacts usually happen when there is difference between surface and surrounding temperatures. Thermal radiation effects on micropolar fluid flow and heat transfer over a porous shrinking sheet is studied by Bhattacharyya et al. [25]. Bhattacharyya [26] analyzed MHD flow of Casson fluid in the presence of radiative stretching sheet in the stagnation region. Hayat et al. [27] investigated the Maxwell flow of mixed convection near a stagnation point along with thermal radiation and convective boundary conditions.

It is now established experimentally as well as theoretically that the mathematical models derived with the help of fractional order derivatives simulate certain physical phenomenon more realistically, particularly for the systems wherein the hereditary effects are important as they depend on the past conditions. Recently fractional models have been developed and employed in many fields of science and engineering like fluid dynamics, electromagnetic, biopopulation models, viscoelasticity, optics, electro-chemistry, and signal processing in order to establish behavior of several physical quantities; see, for example, [28–31] and the references therein. For accurate modeling of damping, fractional models are used; the reader is referred to study the articles [32–35]. Physical phenomena of fluid mechanics, electricity, quantum mechanics models, etc. are controlled within their domain of validity by using integer order partial differential equations [36–38]. Many researchers are using fractional calculus in their research work such as Fetecau et al. [39] who investigated the fractional model of nanofluids with Caputo time derivative and discussed the influence of a fractional parameter on velocity and temperature. Shah et al. [40] studied the Caputo fractional derivative model of a blood flow in a circular cylinder with magnetic particles. Numerical simulations are used to study the behavior of a fractional parameter on fluid and particles velocity. Similarly many authors used fractional calculus in their research work [41–45].

The aim of present study is to investigate the convection effects along with the magnetic field and thermal radiations on the boundary layer flow of fractional Maxwell fluid over a moving plate. The fluid motion is initiated by moving the plate impulsively along the $x - axis$. In order to capture memory effects during the motion of fluid, fractional calculus approach has been employed in order to derive the mathematical model which finally gives fractional coupled nonlinear partial differential equations with mixed time-space variables. The numerical simulations of the underlying model have been carried out by employing a newly developed finite difference method along with $L1$-algorithm. Various flow and fractional parameters effects on velocity and temperature profile are presented via graphs. Moreover, fractional and other physical parameters effects have also been discussed on average skin friction coefficient and average Nusselt number with the help of tables.

2. Mathematical Formulation of the Problem

The incompressible Navier-Stokes equations along with the energy conservation equation have been utilized in order to model the underlying physical phenomenon of two dimensional boundary layer Maxwell flow of nanofluid with heat transfer over a moving surface aligned with $x-axis$. Uniform magnetic field $(0, B_0, 0)$ in the positive $y-$ direction has been introduced in the model using Lorentz force and radiation $\mathbf{q}_r$ has been applied externally while the fluid motion is considered along x coordinate. The velocity field is taken as

$$\mathbf{V} = \left(u\left(x, y, t\right), v\left(x, y, t\right), 0\right) \tag{1}$$

It is to be noted that the viscous dissipation effects are ignored in the derived model. Moreover, the fluid motion along horizontal direction is investigated; therefore the equation of velocity component v is ignored. Using the boundary layer assumptions and Boussinesq approximations, the equations for conservation of mass and momentum for nanofluid in the presence of magnetic field can be written as

$$\frac{\partial u}{\partial x} + \frac{\partial v}{\partial y} = 0, \tag{2}$$

$$\frac{\partial u}{\partial t} + u\frac{\partial u}{\partial x} + v\frac{\partial u}{\partial y} = \nu_{nf}\frac{\partial \tau_{xy}}{\partial y} - \frac{\sigma_{nf}B_0^2}{\rho_{nf}}u - \frac{\nu_{nf}}{k_{nf}}u + \beta_{nf}g\left(T - T_0\right). \tag{3}$$

where nf stands for nanofluid, ν_{nf} is dynamic viscosity, ρ_{nf} is density, β_{nf} is thermal expansion coefficient, k_{nf} is thermal

conductivity, σ_{nf} is electrical conductivity of nanofluid, and g is the gravitational acceleration. The fractional order derivation is introduced into the constitutive equations for the Maxwell model as proposed by Friedrich [46]

$$\tau_{xy} + \lambda_1^{\alpha} \frac{\partial^{\alpha} \tau_{xy}}{\partial t^{\alpha}} = \mu \frac{\partial u}{\partial y}, \tag{4}$$

which leads to

$$\left(1 + \lambda_1^{\alpha} \frac{\partial^{\alpha}}{\partial t^{\alpha}}\right) \tau_{xy} = \mu \frac{\partial u}{\partial y}, \tag{5}$$

where λ_1 is the relaxation time, α is fractional derivative such that $0 < \alpha < 1$, and τ_{xy} is shear stress. The operator $\partial^{\alpha}/\partial t^{\alpha}$ is Caputo time derivative of order α defined as [47]

$$\partial_t^{\alpha} g(t) \coloneqq \frac{1}{\Gamma(n-\alpha)} \int_0^t (t-\xi)^{n-\alpha-1} \frac{\partial^n g(\xi)}{\partial \xi^n} d\xi, \quad n-1 < \Re e\{\alpha\} < n, \ n \in \mathbb{N}, \tag{6}$$

with $\Gamma(\cdot)$ denotes the classical Gamma function given by

$$\Gamma(z) \coloneqq \int_{\mathbb{R}} \xi^{z-1} e^{-\xi} d\xi, \quad z \in \mathbb{C}, \ \Re\{z\} > 0. \tag{7}$$

In order to eliminate τ_{xy} from (3) and (5), applying the operator $(1 + \lambda_1^{\alpha}(\partial^{\alpha}/\partial t^{\alpha}))$ on both sides of (3) and then using (5), we finally arrive at

$$\begin{aligned} &\frac{\partial u}{\partial t} + u\frac{\partial u}{\partial x} + v\frac{\partial u}{\partial y} + \lambda_1^{\alpha}\frac{\partial^{\alpha+1} u}{\partial t^{\alpha+1}} + \lambda_1^{\alpha}\frac{\partial^{\alpha}}{\partial t^{\alpha}}\left(u\frac{\partial u}{\partial x}\right) \\ &\quad + \lambda_1^{\alpha}\frac{\partial^{\alpha}}{\partial t^{\alpha}}\left(v\frac{\partial u}{\partial y}\right) \\ &= \nu_{nf}\frac{\partial^2 u}{\partial y^2} + \beta_{nf} g\left(1 + \lambda_1^{\alpha}\frac{\partial^{\alpha}}{\partial t^{\alpha}}\right)(T - T_0) \\ &\quad - \left(1 + \lambda_1^{\alpha}\frac{\partial^{\alpha}}{\partial t^{\alpha}}\right)\left(\frac{\sigma_{nf} B_0^2}{\rho_{nf}} + \frac{\nu_{nf}}{k_{nf}}\right) u, \end{aligned} \tag{8}$$

The temperature on the plate is presumed to be T_0 and on the surface of the fluid the temperature is considered to be the ambient. The change of temperature within the fluid is modeled by using

$$\frac{\partial T}{\partial t} + u\frac{\partial T}{\partial x} + v\frac{\partial T}{\partial y} = -\nabla \cdot \mathbf{q} - \frac{1}{\left(\rho c_p\right)_{nf}} \frac{\partial \mathbf{q}_r}{\partial y}, \tag{9}$$

where $\mathbf{q}$ is the heat flux, $c_{p_{nf}}$ is heat capacity, and q_r is the thermal radiation. Since the heat flux is supposed to be towards vertical direction, therefore the above equation can further be written as

$$\frac{\partial T}{\partial t} + u\frac{\partial T}{\partial x} + v\frac{\partial T}{\partial y} = -\frac{\partial \mathbf{q}}{\partial y} - \frac{1}{\left(\rho c_p\right)_{nf}} \frac{\partial \mathbf{q}_r}{\partial y}, \tag{10}$$

The expression for $\mathbf{q}$ is given by the fractional form of generalized Fourier's law introduced by Cattaneo [48]

$$\left(1 + \lambda_2^{\gamma} \frac{\partial^{\gamma}}{\partial t^{\gamma}}\right) \mathbf{q} = -k \frac{\partial T}{\partial y}, \tag{11}$$

In order to eliminate $\mathbf{q}$, first applying the operator $(1 + \lambda_2^{\gamma}(\partial^{\gamma}/\partial t^{\alpha}))$ on both sides of (10) and then using (11), we have obtained

$$\begin{aligned} &\frac{\partial T}{\partial t} + u\frac{\partial T}{\partial x} + v\frac{\partial T}{\partial y} + \lambda_2^{\gamma}\frac{\partial^{\gamma+1} T}{\partial t^{\gamma+1}} + \lambda_2^{\gamma}\frac{\partial^{\gamma}}{\partial t^{\gamma}}\left(u\frac{\partial T}{\partial x}\right) \\ &\quad + \lambda_2^{\gamma}\frac{\partial^{\gamma}}{\partial t^{\gamma}}\left(v\frac{\partial T}{\partial y}\right) \\ &= \frac{k_{nf}}{\left(\rho c_p\right)_{nf}}\frac{\partial^2 T}{\partial y^2} - \frac{1}{\left(\rho c_p\right)_{nf}}\left(1 + \lambda_2^{\alpha}\frac{\partial^{\gamma}}{\partial t^{\gamma}}\right)\frac{\partial \mathbf{q}_r}{\partial y}, \end{aligned} \tag{12}$$

where the expression $\mathbf{q}_r$ defined by [49]

$$\mathbf{q}_r = -\frac{4\sigma}{3\beta}\frac{\partial T^4}{\partial y} \tag{13}$$

introduces the radiation contribution in the flow field. Expanding T^4 by a Taylor series about T_0 and neglecting higher orders of T, we can write $T^4 = 4T_0^3 T - 3T_0^4$. Therefore $\mathbf{q}_r$ can eventually be defined as

$$\mathbf{q}_r = -\frac{4\sigma}{3\beta}\frac{\partial T^4}{\partial y} \cong -\frac{16\sigma T_0^3}{3\beta}\frac{\partial T}{\partial y} \tag{14}$$

Using (14) and (11), (12) can be written as

$$\begin{aligned} &\frac{\partial T}{\partial t} + u\frac{\partial T}{\partial x} + v\frac{\partial T}{\partial y} + \lambda_2^{\gamma}\frac{\partial^{\gamma+1} T}{\partial t^{\gamma+1}} + \lambda_2^{\gamma}\frac{\partial^{\gamma}}{\partial t^{\gamma}}\left(u\frac{\partial T}{\partial x}\right) \\ &\quad + \lambda_2^{\gamma}\frac{\partial^{\gamma}}{\partial t^{\gamma}}\left(v\frac{\partial T}{\partial y}\right) \\ &= \left(\frac{k_{nf}}{\left(\rho c_p\right)_{nf}} - \frac{16\sigma T_0^3}{3\beta\left(\rho c_p\right)_{nf}}\right)\frac{\partial^2 T}{\partial y^2}. \end{aligned} \tag{15}$$

Finally, (2), (8), and (15) constitute the model problem which describes the underlying physical phenomenon addressed in this work

$$\begin{aligned}
&\frac{\partial u}{\partial x}+\frac{\partial v}{\partial y}=0,\\
&\frac{\partial u}{\partial t}+u\frac{\partial u}{\partial x}+v\frac{\partial u}{\partial y}+\lambda_1^{\alpha}\frac{\partial^{\alpha+1}u}{\partial t^{\alpha+1}}+\lambda_1^{\alpha}\frac{\partial^{\alpha}}{\partial t^{\alpha}}\left(u\frac{\partial u}{\partial x}\right)\\
&\quad+\lambda_1^{\alpha}\frac{\partial^{\alpha}}{\partial t^{\alpha}}\left(v\frac{\partial u}{\partial y}\right)=\nu_{nf}\frac{\partial^2 u}{\partial y^2}\\
&\quad+\beta_{nf}g\left(1+\lambda_1^{\alpha}\frac{\partial^{\alpha}}{\partial t^{\alpha}}\right)(T-T_0)\\
&\quad-B_1^2\left(1+\lambda_1^{\alpha}\frac{\partial^{\alpha}}{\partial t^{\alpha}}\right)u,\\
&\frac{\partial T}{\partial t}+u\frac{\partial T}{\partial x}+v\frac{\partial T}{\partial y}+\lambda_2^{\gamma}\frac{\partial^{\gamma+1}T}{\partial t^{\gamma+1}}+\lambda_2^{\gamma}\frac{\partial^{\gamma}}{\partial t^{\gamma}}\left(u\frac{\partial T}{\partial x}\right)\\
&\quad+\lambda_2^{\gamma}\frac{\partial^{\gamma}}{\partial t^{\gamma}}\left(v\frac{\partial T}{\partial y}\right)=K_{nf}^1\frac{\partial^2 T}{\partial y^2}.
\end{aligned}\tag{16}$$

where

$$\begin{aligned}
B_1^2&=\left(\frac{\sigma_{nf}B_0^2}{\rho_{nf}}+\frac{\nu_{nf}}{k_{nf}}\right),\\
K_{nf}^1&=\left(\frac{k_{nf}}{\left(\rho c_p\right)_{nf}}-\frac{16\sigma T_0^3}{3\beta\left(\rho c_p\right)_{nf}}\right)
\end{aligned}\tag{17}$$

and ρ_{nf} is density of nanofluid, μ_{nf} is dynamic viscosity of nanofluid, and other parameters for the nanofluid are defined as [50]

$$\begin{aligned}
\rho_{nf}&=(1-\phi)\rho_{nf}+\phi\rho_s,\\
\frac{k_{nf}}{k_f}&=\left(\frac{k_s+2k_f-2\phi\left(k_f-k_s\right)}{k_s+2k_f+\phi\left(k_f-k_s\right)}\right),\\
(\rho\beta)_n f&=(1-\phi)(\rho\beta)_f+\phi(\rho\beta)_s,\\
\sigma_{nf}&=k_f(1+(\sigma-1)\phi),\\
\left(\rho c_p\right)_{nf}&=\phi\left(\rho c_p\right)_s+(1-\phi)\left(\rho c_p\right)_f,\\
\mu_{nf}&=\frac{\mu_f}{(1-\phi)^{2.5}}.
\end{aligned}\tag{18}$$

In the above equations, ϕ denotes the volume fraction of the nanoparticles in nanofluid. ρ_s, k_s, μ_s, and $(c_p)_s$ denote density, thermal conductivity, viscosity, and specific heat capacities of surfactant respectively. Similarly ρ_f, k_f, and $(c_p)_f$ denote density, thermal conductivity, and specific heat capacities of base fluid, respectively.

As described earlier, the fluid motion at time $t = 0$ is initiated by an impulsive movement of the plate with the time dependent velocity tU_0; the temperature of the plate is also dependent on time t; therefore the initial and boundary conditions which best suit the physical phenomenon can be given by

$$\begin{aligned}
&t\leqslant 0: v=0,\\
&u=0,\\
&T=0,\\
&t>0: v=0,\\
&u=0,\\
&T=0\\
&\qquad\qquad at\ x=0,\\
&t>0: u=tU_0,\\
&T=\frac{T_d-T_0}{T_0}t\\
&\qquad\qquad at\ y=0,\\
&t>0: u\longrightarrow 0,\\
&T\longrightarrow T_0\\
&\qquad\qquad at\ y\longrightarrow\infty.
\end{aligned}\tag{19}$$

2.1. Nondimensionalization. In order to understand physics of the proposed problem in an easy way we have nondimensionalized the governing problem. It helps to comprehend the underlying physical phenomenon with nondimensional parameters of interest without giving any weightage to units of involved quantities. Nondimensionalization of model (16) and (19) can be obtained by considering the following nondimensional variables and parameters:

$$\begin{aligned}
t^*&=\frac{t\nu}{d^2},\\
y^*&=\frac{y}{d},\\
x^*&=\frac{x\nu}{d^2U_0},\\
u^*&=\frac{u}{U_0},\\
v^*&=\frac{dv}{\nu},\\
\lambda_1^*&=\lambda_1\left(\frac{\nu}{d^2}\right),\\
\lambda_2^*&=\lambda_2\left(\frac{\nu}{d^2}\right),\\
\theta&=\frac{T-T_0}{T_d-T_0}
\end{aligned}\tag{20}$$

with the use of chain rule

$$\frac{\partial u}{\partial t} = U_0 \frac{\partial u^*}{\partial t^*} \frac{\partial t^*}{\partial t},$$
$$\frac{\partial u}{\partial y} = U_0 \frac{\partial u^*}{\partial y^*} \frac{\partial y^*}{\partial y}, \tag{21}$$
$$\frac{\partial^\alpha u}{\partial t^\alpha} = U_0 \frac{\nu^\alpha}{d^{2\alpha}} \frac{\partial^\alpha u^*}{\partial t^{*\alpha}}.$$

Using above expressions, model (16) and (19) takes the following form (after removing the asterisk $(*)$ sign):

$$\frac{\partial u}{\partial x} + \frac{\partial v}{\partial y} = 0,$$
$$\frac{\partial u}{\partial t} + u\frac{\partial u}{\partial x} + v\frac{\partial u}{\partial y} + \lambda_1^\alpha \frac{\partial^{\alpha+1} u}{\partial t^{\alpha+1}} + \lambda_1^\alpha \frac{\partial^\alpha}{\partial t^\alpha}\left(u\frac{\partial u}{\partial x}\right) + \lambda_1^\alpha \frac{\partial^\alpha}{\partial t^\alpha}\left(v\frac{\partial u}{\partial y}\right) = \frac{\partial^2 u}{\partial y^2} + G_r \lambda_1^\alpha \frac{\partial^\alpha}{\partial t^\alpha}\theta + G_r\theta - (M + \Phi_2)\, u - (M + \Phi_2)\, \lambda_1^\alpha \frac{\partial^\alpha u}{\partial t^\alpha}, \tag{22}$$
$$\frac{\partial \theta}{\partial t} + u\frac{\partial \theta}{\partial x} + v\frac{\partial \theta}{\partial y} + \lambda_2^\gamma \frac{\partial^{\gamma+1}\theta}{\partial t^{\gamma+1}} + \lambda_2^\gamma \frac{\partial^\gamma}{\partial t^\gamma}\left(u\frac{\partial \theta}{\partial x}\right) + \lambda_2^\gamma \frac{\partial^\gamma}{\partial t^\gamma}\left(v\frac{\partial \theta}{\partial y}\right) = \left(\frac{1 - \Phi_3}{P_r}\right)\frac{\partial^2 \theta}{\partial y^2}.$$

$\Phi_2 = d^2/U_0 \nu k_{nf}$, $\Phi_3 = -16T_0^3(T_d - T_0)\sigma/3\beta(\rho C_p)_{nf} k_{nf}$, $M = \sigma_{nf} B_0^2 d^2/U_0 \nu \mu_{nf}$, $G_r = \beta_{nf} g(T_d - T_0)d^2/U_0 \nu$ Grashof number, and $P_r = U_0 \nu c_p \mu/k d^2$ Prandtl number, respectively.

Dimensionless form of boundary and initial conditions are

$$\begin{aligned}
&t \leqslant 0 : v = 0,\\
&u = 0,\\
&\theta = 0,\\
&t > 0 : v = 0,\\
&u = 0,\\
&\theta = 0 \qquad at\ x = 0,\\
&t > 0 : u = t,\\
&\theta = t \qquad at\ y = 0,\\
&t > 0 : u \longrightarrow 0,\\
&\theta \longrightarrow 0 \qquad at\ y \longrightarrow \infty.
\end{aligned} \tag{23}$$

The subsequent section elucidates the numerical scheme employed to solve the nondimensional mathematical model derived in this section.

3. Numerical Method

This section elucidates briefly the numerical scheme employed to solve the developed model (22)-(23). The finite difference approximations have been utilized along with L_1 scheme in order to discretize the mixed fractional derivatives which appears in the model. Other numerical schemes can also be utilized in order to solve model (22)-(23); for example, V. E. Lynch et al. [51] have discussed two numerical schemes, namely, $L2$ and $L2C$, for solving partial differential equations of fractional order. The authors have investigated explicit and semi-implicit techniques along with two types of discretization schemes. It is found that these techniques depend on the correct choice of discretization methods as well as on the choice of α. The $L2$ scheme demonstrates good convergence results for $\alpha > 1.5$ whereas $L2C$ shows adequate convergence for $\alpha < 1.5$.

$L1$ scheme is a newly introduced technique by F. Liu et. al. [52] wherein the authors have devised a method of discretizing the nonlinear convection terms as well as the terms which involve fractional order derivative of nonlinear terms using finite difference approximations. The $L1$ scheme does not depend on the particular choice of discretization or on the values of fractional order α. The technique has been successfully applied on various models and obtained significant results; see, for example, [3, 53] and references therein. The $L1$ scheme is best suited for the problems of the type considered in this manuscript. The scheme is described briefly in the subsequent section.

3.1. Discretization Method. Define $t_k = k\Delta t$, $k = 0, 1, 2, 3, \ldots, r$, time steps with Δt being a time step size and $x_i = i\Delta x$, $i = 0, 1, 2, 3, \ldots, m$; $y_j = j\Delta y$, $j = 0, 1, 2, 3, \ldots, n$, where $\Delta x = L_x/m$ and $\Delta y = L_y/n$ are space step sizes. Let u_{ij}^k and θ_{ij}^k be numerical approximations of $u(t, x, y)$ and $\theta(t, x, y)$ at point (x_i, y_j) and time t_k in model (22)-(23).

The Caputo time fractional derivative in (6) is discretized at time t_k as follows:

$$\partial_t^\alpha u(t_k) = \frac{1}{\Gamma(2-\alpha)} \sum_{s=0}^{k} \int_{t_k}^{t_{k+1}} (t_k - \xi)^{1-\alpha-1} \frac{\partial u(\xi)}{\partial \xi} d\xi, \qquad 0 < \Re e\{\alpha\} < 1,$$
$$= \frac{\Delta t^{-\alpha}}{\Gamma(2-\alpha)} \left[b_0 u(t_k) - b_{k-1} u(t_0) + \sum_{s=1}^{k-1} (b_{s-1} - b_s)\, u(t_{k-s}) \right] + O(\Delta t) \tag{24}$$

where $b_s = (s)^{1-\alpha} - (s-1)^{1-\alpha}$, $s = 0, 1, 2, \ldots, r$.

The nonfractional derivatives are discretized using backward finite difference approximations as [52, 54]

$$\begin{aligned}
&\left.\frac{\partial u}{\partial t}\right|_{t=t_k} = \frac{u\left(x_i, y_j, t_k\right) - u\left(x_i, y_j, t_{k-1}\right)}{\Delta t} + O\left(\Delta t\right),\\
&\left.u\frac{\partial u}{\partial x}\right|_{t=t_k}\\
&\quad = u\left(x_i, y_j, t_{k-1}\right)\frac{u\left(x_i, y_j, t_k\right) - u\left(x_{i-1}, y_j, t_k\right)}{\Delta x}\\
&\qquad + O\left(\Delta x\right),\\
&\left.v\frac{\partial u}{\partial y}\right|_{t=t_k}\\
&\quad = v\left(x_i, y_j, t_{k-1}\right)\frac{u\left(x_i, y_j, t_k\right) - u\left(x_i, y_{j-1}, t_k\right)}{\Delta y}\\
&\qquad + O\left(\Delta y\right),\\
&\frac{\partial^2 u}{\partial y^2}\\
&\quad = \frac{u_{i,j+1}^k - 2u_{i,j}^k + u_{i,j-1}^k + u_{i,j+1}^{k-1} - 2u_{i,j}^{k-1} + u_{i,j-1}^{k-1}}{2\Delta y}\\
&\qquad + O\left(\Delta y^2\right)
\end{aligned} \tag{25}$$

where $u_{i,j}^k = u(x_i, y_j, t_k)$ and the nonlinear terms have been linearized. Moreover the fractional derivatives of the above terms at time t_k can be defined in the following way (see for details [52]):

$$\begin{aligned}
&\frac{\partial^{\alpha+1} u\left(t_k\right)}{\partial t^{\alpha+1}} = \frac{\Delta t^{-1-\alpha}}{\Gamma\left(2-\alpha\right)}\left[u_{ij}^k - u_{ij}^{k-1}\right.\\
&\qquad \left. - \sum_{s=1}^{k-1}\left(b_{s-1} - b_s\right)\left(u_{ij}^{k-s} - u_{ij}^{k-s-1}\right)\right],\\
&\frac{\partial^{\alpha}}{\partial t^{\alpha}}\left(u\frac{\partial u}{\partial x}\right) = \frac{\Delta t^{-\alpha}}{\Delta x\Gamma\left(2-\alpha\right)}\left[u_{ij}^{k-1}\left(u_{ij}^k - u_{i-1j}^k\right)\right.\\
&\qquad \left. - \sum_{s=1}^{k-1}\left(b_{s-1} - b_s\right)u_{ij}^{k-s-1}\left(u_{ij}^{k-s} - u_{i-1j}^{k-s}\right)\right],\\
&\frac{\partial^{\alpha}}{\partial t^{\alpha}}\left(v\frac{\partial u}{\partial y}\right) = \frac{\Delta t^{-\alpha}}{\Delta y\Gamma\left(2-\alpha\right)}\left[v_{ij}^{k-1}\left(u_{ij+1}^k - u_{ij}^k\right)\right.\\
&\qquad \left. - \sum_{s=1}^{k-1}\left(b_{s-1} - b_s\right)v_{ij}^{k-s-1}\left(u_{ij+1}^{k-s} - u_{ij}^{k-s}\right)\right],
\end{aligned} \tag{26}$$

Assume that

$$\begin{aligned}
\delta_1 &= \lambda^{\alpha}\frac{\Delta t^{-\alpha}}{\Gamma\left(2-\alpha\right)},\\
\delta_2 &= \frac{1}{2\Delta y^2},\\
\delta_3 &= \lambda^{\gamma}\frac{\Delta t^{-\gamma}}{\Gamma\left(2-\gamma\right)},
\end{aligned} \tag{27}$$

and in order to simplify notations, we write

$$\begin{aligned}
A_1 &= \sum_{s=1}^{k-1}\left(b_{s-1} - b_s\right)\left(u_{ij}^{k-s} - u_{ij}^{k-s-1}\right),\\
A_2 &= \sum_{s=1}^{k-1}\left(b_{s-1} - b_s\right)u_{ij}^{k-s-1}\left(u_{ij}^{k-s} - u_{i-1j}^{k-s}\right),\\
A_3 &= \sum_{s=1}^{k-1}\left(b_{s-1} - b_s\right)v_{ij}^{k-s-1}\left(u_{ij+1}^{k-s} - u_{ij}^{k-s}\right),\\
A_4 &= \theta_{ij}^{k-1} - \sum_{s=1}^{k-1}\left(b_{s-1} - b_s\right)\theta_{ij}^{k-s},\\
A_5 &= -\sum_{s=1}^{k-1}\left(b_{s-1} - b_s\right)u_{ij}^{k-s}.
\end{aligned} \tag{28}$$

By using similar conventions, we can easily obtain the approximations for the fractional derivatives terms involved in the temperature equation given below

$$\begin{aligned}
&\frac{\partial^{\alpha+1}\theta\left(t_k\right)}{\partial t^{\alpha+1}} = \frac{\Delta t^{-1-\alpha}}{\Gamma\left(2-\alpha\right)}\left[\theta_{ij}^k - \theta_{ij}^{k-1}\right.\\
&\qquad \left. - \sum_{s=1}^{k-1}\left(c_{s-1} - c_s\right)\left(\theta_{ij}^{k-s} - \theta_{ij}^{k-s-1}\right)\right],\\
&\frac{\partial^{\alpha}}{\partial t^{\alpha}}\left(u\frac{\partial\theta}{\partial x}\right) = \frac{\Delta t^{-\alpha}}{\Delta x\Gamma\left(2-\alpha\right)}\left[u_{ij}^{k-1}\left(\theta_{ij}^k - \theta_{i-1j}^k\right)\right.\\
&\qquad \left. - \sum_{s=1}^{k-1}\left(c_{s-1} - c_s\right)u_{ij}^{k-s-1}\left(\theta_{ij}^{k-s} - \theta_{i-1j}^{k-s}\right)\right],\\
&\frac{\partial^{\alpha}}{\partial t^{\alpha}}\left(v\frac{\partial\theta}{\partial y}\right) = \frac{\Delta t^{-\alpha}}{\Delta y\Gamma\left(2-\alpha\right)}\left[v_{ij}^{k-1}\left(\theta_{ij+1}^k - \theta_{ij}^k\right)\right.\\
&\qquad \left. - \sum_{s=1}^{k-1}\left(c_{s-1} - c_s\right)v_{ij}^{k-s-1}\left(\theta_{ij+1}^{k-s} - \theta_{ij}^{k-s}\right)\right],
\end{aligned} \tag{29}$$

where $c_s = (s)^{1-\alpha} - (s-1)^{1-\alpha}$, $s = 0, 1, 2, \ldots, r$. In order to simplify the notations, we assume that

$$B_1 = \sum_{s=1}^{k-1} \left(c_{s-1} - c_s\right)\left(\theta_{ij}^{k-s} - \theta_{ij}^{k-s-1}\right),$$

$$B_2 = \sum_{s=1}^{k-1} \left(c_{s-1} - c_s\right) u_{ij}^{k-s-1}\left(\theta_{ij}^{k-s} - \theta_{i-1j}^{k-s}\right), \tag{30}$$

$$B_3 = \sum_{s=1}^{k-1} \left(c_{s-1} - c_s\right) v_{ij}^{k-s-1}\left(\theta_{ij+1}^{k-s} - \theta_{ij}^{k-s}\right),$$

Finally, by substituting approximations (25)-(30) in the model equations (22), we can obtain the following discretization scheme:

$$\begin{aligned} v_{ij}^k &= v_{ij-1}^k + v_{ij-1}^{k-1} - v_{ij}^{k-1} + 2\frac{h_y}{h_x}\left(u_{i-1j-1}^{k-1} - u_{ij-1}^{k-1} + u_{i-1j}^{k-1}\right. \\ &\quad \left. - u_{ij}^{k-1} + u_{i-1j-1}^{k} - u_{ij-1}^{k} + u_{i-1j}^{k} - u_{ij}^{k}\right), \end{aligned} \tag{31}$$

$$\begin{aligned} u_{ij}^k &\left(\frac{1}{\Delta t} + \frac{u_{ij}^{k-1}}{\Delta x} + \frac{v_{ij}^{k-1}}{\Delta y} + \frac{\delta_1}{\Delta t} + u_{ij}^{k-1}\frac{\delta_1}{\Delta x} - v_{ij}^{k-1}\frac{\delta_1}{\Delta y}\right. \\ &\left. + 2\delta_2 + \left(M + \Phi_2\right)\left(1 + \frac{\delta_1}{\Delta t}\right)\right) + u_{i-1j}^{k}\left(-\frac{u_{ij}^{k-1}}{\Delta x}\right. \\ &\left. - u_{ij}^{k-1}\frac{\delta_1}{\Delta x}\right) + u_{ij-1}^{k}\left(-\frac{v_{ij}^{k-1}}{\Delta y} - \delta_2\right) + u_{ij+1}^{k}\left(-\delta_2\right. \\ &\left. + \frac{\delta_1 v_{ij}^{k-1}}{\Delta y}\right) = u_{ij}^{k-1}\left(\frac{1}{\Delta t} + \frac{\delta_1}{\Delta t} - 2\delta_2\right) + \frac{\delta_1}{\Delta t}A_1 \\ &+ \frac{\delta_1}{\Delta x}A_2 + \frac{\delta_1}{\Delta y}A_3 + \delta_2 u_{ij+1}^{k-1} + \delta_2 u_{ij-1}^{k-1} + \delta_1 G_r A_4 \\ &+ G_r\theta_{ij}^{k-1} + \left(M + \phi_2\right)\delta_1 A_5, \end{aligned} \tag{32}$$

$$\begin{aligned} \theta_{ij}^k &\left(\frac{1}{\Delta t} + u_{ij}^{k-1}\frac{1}{\Delta x} + v_{ij}^{k-1}\frac{1}{\Delta y} + \delta_3\frac{1}{\Delta t} + \delta_3 u_{ij}^{k-1}\frac{1}{\Delta x}\right. \\ &\left. + \delta_3 v_{ij}^{k-1}\frac{1}{\Delta y} + \delta_2\frac{2}{p_r}\left(1 - \phi_3\right)\right) + \theta_{i-1j}^{k}\left(-\frac{u_{ij}^{k-1}}{\Delta x}\right. \\ &\left. - \frac{\delta_3}{\Delta x}u_{ij}^{k-1}\right) + \theta_{ij-1}^{k}\left(-\frac{v_{ij}^{k-1}}{\Delta y} - \frac{\delta_3}{\Delta y}v_{ij}^{k-1}\right. \\ &\left. - \frac{\delta_2}{P_r}\left(1 - \phi_3\right)\right) - \frac{\delta_2}{P_r}\left(1 - \phi_3\right)\theta_{ij+1}^{k} = \theta_{ij}^{k-1}\left(\frac{1}{\Delta t}\right. \\ &\left. + \delta_3\frac{1}{\Delta t} - 2\frac{\delta_2}{P_r}\left(1 - \phi_3\right)\right) + \delta_3\left(B_1\frac{1}{\Delta t} + B_2\frac{1}{\Delta x}\right. \\ &\left. + B_3\frac{1}{\Delta y}\right) + \frac{\delta_2}{P_r}\left(1 - \phi_3\right)\left(\theta_{ij+1}^{k-1} + \theta_{ij-1}^{k-1}\right), \end{aligned} \tag{33}$$

and the initial and boundary conditions can evidently be defined as

$$\begin{aligned} v_{ij}^0 &= 0, \\ u_{ij}^0 &= 0, \\ \theta_{ij}^0 &= 0, \\ v_{0j}^k &= 0, \\ u_{0j}^k &= 0, \\ \theta_{0j}^k &= 0, \\ v_{i0}^k &= 0, \\ u_{i0}^k &= t_k, \\ \theta_{i0}^k &= 0, \\ v_{iL_y}^k &= 0, \\ u_{iL_y}^k &= 0, \\ \theta_{iL_y}^k &= 0. \end{aligned} \tag{34}$$

3.2. Solution Procedure. The computational domain is considered as a rectangle with sizes $L_x = 1$ and $L_y = 5$ where L_y corresponds to $y \longrightarrow \infty$ as the solution approaches to zeros in the vicinity of $L_y = 5$; see Figure 5 for validation. The solution has been computed with mesh sizes $\Delta x = 0.01$, $\Delta y = 0.01$, and $\Delta t = 0.01$. The iteration process in the numerical scheme (31)-(33) has been initiated by initial values u_{ij}^0, v_{ij}^0, and θ_{ij}^0 given by (34). Assuming that the earlier values u_{ij}^{k-1}, v_{ij}^{k-1}, and θ_{ij}^{k-1} at time $t = t_{k-1}$ are known for the $k-level$ iteration. The memory terms A_1, A_2, A_3 and B_1, B_2, B_3 are also known as these terms are defined till the $(k-1)th$ time step. Finally, the iteration at each kth time step can be written in the form of five diagonal linear systems by placing each term of $(k-1)th$ step on the right hand side of the systems. The linear systems are then solved by using a classical direct method. A code has been developed in MATLAB in order to implement scheme (31)-(34).

4. Skin Friction Coefficient

The fluid layer adjacent to the boundary (plate) is characterized by the skin friction coefficient or shear stress coefficient denoted as $\mathscr{C}_f$ and defined by [53]

$$\mathscr{C}_f = \frac{\mu_{nf}}{\rho_f U_0^2}\tau_w, \tag{35}$$

with the stress at the boundary being defined by

$$\tau_w = \left.\frac{\partial u}{\partial y}\right|_{y=0}, \tag{36}$$

whereas the fractional form of the stress can be defined using (5) as

$$\left(1+\lambda_1^{\alpha}\frac{\partial^{\alpha}}{\partial t^{\alpha}}\right)\tau_w=\left.\frac{\partial u}{\partial y}\right|_{y=0}, \tag{37}$$

Applying operator $(1+\lambda_1^{\alpha}(\partial^{\alpha}/\partial t^{\alpha}))$ on both sides of (35) and using (37), the skin friction coefficient $\mathscr{C}_f$ can finally be defined as

$$\left(1+\lambda_1^{\alpha}\frac{\partial^{\alpha}}{\partial t^{\alpha}}\right)\mathscr{C}_f=\left.\frac{\mu_{nf}}{\rho_f U_0^2}\frac{\partial u}{\partial y}\right|_{y=0}, \tag{38}$$

Using the nondimensional quantities defined in Section 2.1, the dimensionless form of the skin friction is given by

$$\left(1+\lambda_1^{\alpha}\frac{\partial^{\alpha}}{\partial t^{\alpha}}\right)\mathscr{C}_f=\left.\frac{1}{Re}\frac{\partial u}{\partial y}\right|_{y=0}, \tag{39}$$

Using $L1$-discretization of Caputo derivative defined in (24), the skin friction coefficient $\mathscr{C}_f$ can be written as

$$\mathscr{C}_f=\frac{\delta_1\sum_{s=1}^{k-1}(b_{s-1}-b_s)\,\mathscr{C}_f(t_{k-s})+(1/Re)\left.(\partial u/\partial y)\right|_{y=0}}{1+\delta_1} \tag{40}$$

where $Re=U_0d/\nu$ is the Reynolds number. The average skin friction coefficient can further be defined as

$$\overline{\mathscr{C}_f}=\frac{\delta_1\sum_{s=1}^{k-1}(b_{s-1}-b_s)\,\overline{\mathscr{C}_f}(t_{k-s})+(1/Re)\int_0^1\left.(\partial u/\partial y)\right|_{y=0}dx}{1+\delta_1} \tag{41}$$

The skin friction coefficient has been calculated for different values of physical parameters and the results have been shown in Table 1.

5. Local Nusselt Number

A ratio between convective and conductive heat transfer in the fluid is known as local Nusselt number denoted by Nu. The large values of the Nusselt number show the dominated heat transfer by convection in the fluid. The Nusselt number for Maxwell fluid is [53]

$$Nu=-\frac{dk_{nf}}{k_f(T_d-T_0)}\mathbf{q}_w, \tag{42}$$

with the expression for $\mathbf{q}_w$ defined by

$$\mathbf{q}_w=\left.\frac{\partial T}{\partial y}\right|_{y=0} \tag{43}$$

and for the fractional Maxwell fluid, we can define (see for details [29])

$$\left(1+\lambda_2^{\alpha}\frac{\partial^{\alpha}}{\partial t^{\alpha}}\right)\mathbf{q}_w=\left.\frac{\partial T}{\partial y}\right|_{y=0} \tag{44}$$

Table 1: Average skin friction coefficient for different parameters.

α	λ_1	M	Φ_2	$\overline{Cf}$
0.1	0.2	0.01	0.01	-8.2201
0.3	0.2	0.01	0.01	-9.3333
0.6	0.2	0.01	0.01	-10.5056
0.9	0.2	0.01	0.01	-11.1255
0.1	**0.2**	0.01	0.01	-8.2201
0.1	**0.4**	0.01	0.01	-8.0712
0.1	**0.6**	0.01	0.01	-7.9827
0.1	**0.8**	0.01	0.01	-7.9193
0.1	0.2	**0.01**	0.01	-8.2201
0.1	0.2	**0.05**	0.01	-8.2399
0.1	0.2	**0.1**	0.01	-8.2647
0.1	0.2	**0.5**	0.01	-8.4069
0.1	0.2	0.01	**0.01**	-8.2201
0.1	0.2	0.01	**0.1**	-8.2647
0.1	0.2	0.01	**1.1**	-8.7495
0.1	0.2	0.01	**2.1**	-9.2150

Applying operator $(1+\lambda_2^{\gamma}(\partial^{\gamma}/\partial t^{\gamma}))$ on both sides of (42) and using above relations, the Nusselt number Nu can be written as

$$\left(1+\lambda_2^{\alpha}\frac{\partial^{\gamma}}{\partial t^{\gamma}}\right)Nu=-\frac{dk_{nf}}{k_f(T_d-T_0)}\left.\frac{\partial T}{\partial y}\right|_{y=0} \tag{45}$$

The dimensionless form of Nussult number can be defined using relations in Section 2.1 as

$$\left(1+\lambda_2^{\gamma}\frac{\partial^{\gamma}}{\partial t^{\gamma}}\right)Nu=-\frac{k_{nf}}{k_f}\left.\frac{\partial\theta}{\partial y}\right|_{y=0} \tag{46}$$

Using $L1$-discretization of Caputo derivative defined in (24), the Nusselt number Nu can be discretized as

$$Nu=\frac{\delta_3\sum_{s=1}^{k-1}(c_{s-1}-c_s)\,Nu(t_{k-s})-\left(k_{nf}/k_f\right)\left.(\partial\theta/\partial y)\right|_{y=0}}{1+\delta_3} \tag{47}$$

Moreover, the average Nusselt number can be given as

$$\overline{Nu}=\frac{\delta_3\sum_{s=1}^{k-1}(c_{s-1}-c_s)\,\overline{Nu}(t_{k-s})-\left(k_{nf}/k_f\right)\int_0^1\left.(\partial\theta/\partial y)\right|_{y=0}dx}{1+\delta_3} \tag{48}$$

The Nusselt number has been calculated for various values of physical quantities and the outcomes have been shown in Table 2.

6. Results and Discussion

In this section, the effects of heat transfer flow of fractional Maxwell fluid with magnetic field and radiation over a moving plate are studied. The nonlinear coupled equations

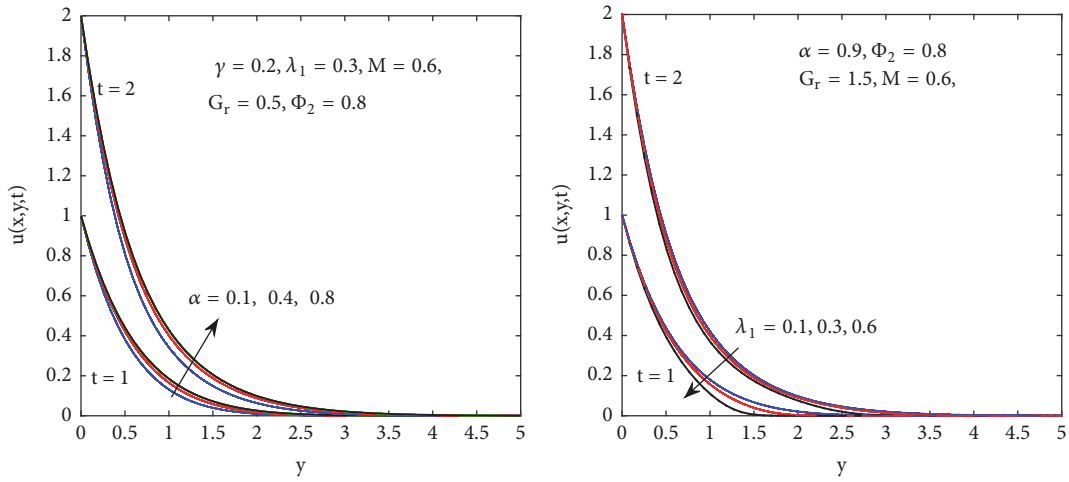

(a) Velocity distribution with α variation

(b) Velocity distribution for λ_1

Figure 1

Table 2: Average Nusselt number for different parameters.

γ	λ_2	P_r	Φ_3	$\overline{Nu}$
0.1	0.2	0.01	0.01	-52.0576
0.3	0.2	0.01	0.01	-76.5177
0.6	0.2	0.01	0.01	-1.9658e+02
0.9	0.2	0.01	0.01	-1.1654e+03
0.1	**0.2**	0.01	0.01	-52.0576
0.1	**0.4**	0.01	0.01	-51.4028
0.1	**0.6**	0.01	0.01	-51.0632
0.1	**01**	0.01	0.01	-50.6861
0.1	0.2	**0.01**	0.01	-52.0576
0.1	0.2	**0.05**	0.01	-52.1020
0.1	0.2	**0.09**	0.01	–52.1483
0.1	0.2	**0.1**	0.01	–52.1594
0.1	0.2	0.01	**0.01**	-52.0576
0.1	0.2	0.01	**0.05**	-52.0518
0.1	0.2	0.01	**0.1**	-52.0466
0.1	0.2	0.01	**0.5**	-52.0193

are numerically solved by newly developed $L1$ technique along with the finite difference approximations as described earlier. The parameters involved in the model which are discussed are mainly the fractional parameters α, γ, Maxwell or the relaxation time parameters λ_1, λ_2, Prandtl number P_r, magnetic field M, radiation parameter Φ_3, and nanofluid parameter Φ_2. The effects of these parameters on the velocity and temperature profiles along with skin friction coefficient $\mathscr{C}_f$ and Nusselt number Nu have been investigated and explained via graphs and tables.

6.1. Effects on Velocity Field. Figure 1(a) indicates that fractional parameter α effects on velocity profile with final time $t_f = 1$ and $t_f = 2$. For grater values of α, the velocity of the fluid increases. This implies that increase in the fractional parameter α gives rise in the thickness of velocity for the both short and long times. However this dependence is indeed nonmonotonic in behavior and cannot be generalized to all values of the involved parameters as for the cases discussed here. Change in behavior can be noted for some other values of involved parameters. Similar pattern can be seen for boundary layer thickness of the flow domain.

Figure 1(b) shows relaxation time λ_1 effects on velocity profile. Velocity of the fluid decreases for larger values of λ_1. For time $t_f = 1$, velocity of the fluid decreases quickly when we have larger values of λ_1. It is perceived that velocity profile decreases while corresponding boundary layer thickness increases with the increase of λ_1. The parameter λ_1 appeared in nondimensional momentum equation due to dimensional relaxation time. The relaxation time is stronger for larger λ_1. Hence velocity profile decreases by the increase of λ_1. Influence of magnetic field on fluid velocity is shown in Figure 2(a). The increase of magnetic field parameter M tends to decrease velocity profile. The Lorentz force increases with the increase of magnetic number which offers resistance to the motion of fluid. Therefore magnitude of the skin friction coefficient and velocity profile decreases. Effects of nanoparticles volume ϕ on nanofluids are shown in Figure 2(b). The increase in the volumic concentration ϕ of nanoparticles decreases velocity which is physically adequate as observed in experimental findings.

6.2. Effects on Temperature Field. Dimensionless form of a temperature is considered because of the fact that the natural convection is driven by temperature gradient. Figure 3(a) demonstrates that fractional parameter effect of γ on temperature is the same like in α case on velocity profile. Decreasing γ values from 1 to 0 quickly decreases temperature. This shows that noninteger order derivatives weaken the effects of heat conduction. Relaxation time parameter λ_2 effects on temperature field are shown in Figure 3(b). A small change occurs in temperature for small values of λ_2. Petit increase in λ_2 decreases temperature profile slightly. Radiation effects on temperature profile are shown in Figure 4(a). Radiation

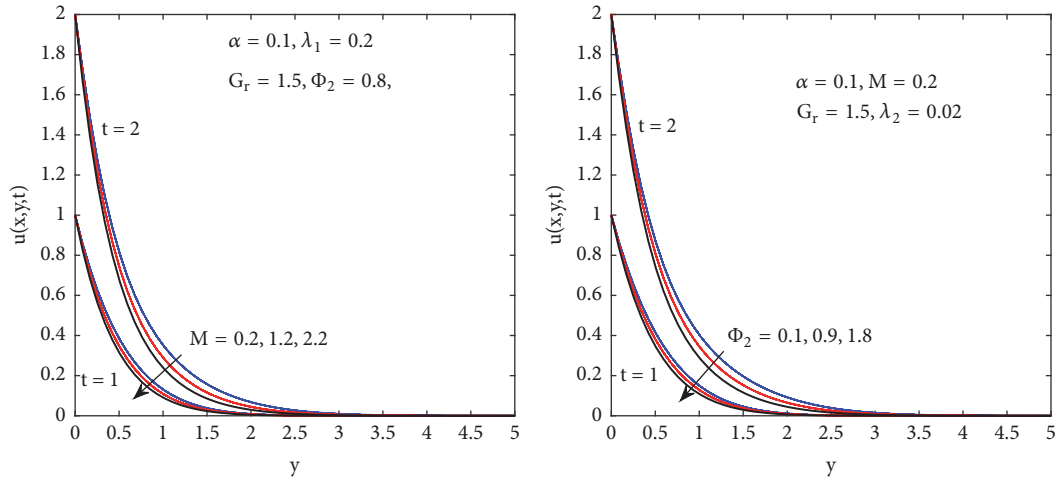

(a) Velocity distribution for M (b) Velocity distribution for Φ_2

Figure 2

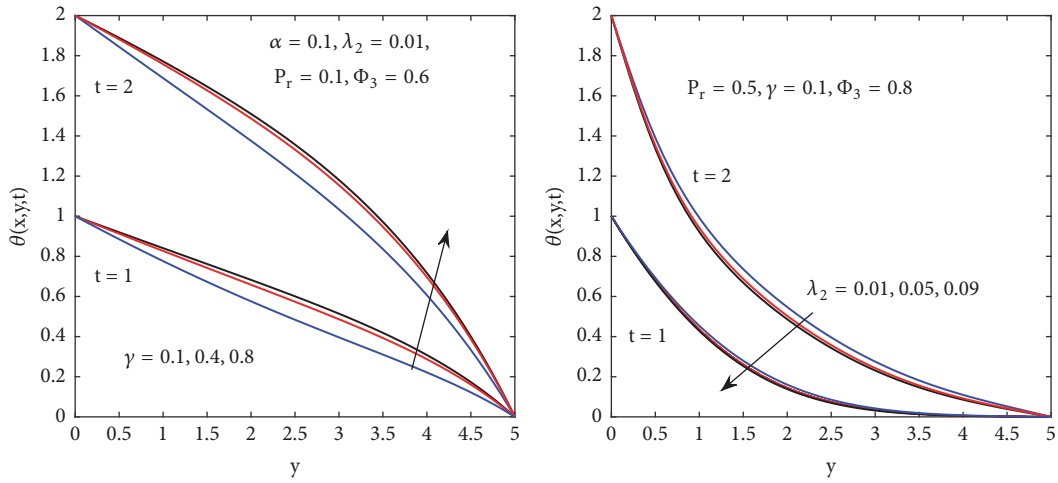

(a) Temperature distributions with γ variation (b) Temperature distribution for λ_2

Figure 3

parameter Φ_3 minor increment makes a larger change in temperature field. Prandtl number is defined as the ratio of momentum diffusivity by thermal diffusivity. Prandtl number Pr effects on temperature are shown in Figure 4(b). A petit increase in Prandtl number demonstrates decrease in temperature profile. Also note that thermal boundary layer thickness is at lower level for larger values of Pr. With the increase of Pr momentum diffusivity increases. Hence with the increase of Pr thermal diffusivity decreases while viscosity of fluid increases, as a result temperature and velocity profiles decrease. Relative thickness of thermal and momentum boundary layers is controlled by Pr. Heat diffuses gradually and thermal boundary layer is at lower level for larger values of Pr while opposite behavior is observed at smaller values of Pr.

Figures 5(a) and 5(b) show three-dimensional velocity and temperature distribution which demonstrate convergence and good stability in space and time variables. The particular values of α and γ are the Caputo fractional derivatives which vary from 0 to 1. As derivative of order zero makes no sense for the proposed physical problem and the derivative of order 1 will reduce the proposed model to the classical one. The values of λ_1 and λ_2 are the relaxation times for momentum and heat equations, respectively. We have to consider the values of these parameters greater than zero as for zero there is no contribution of relaxation times and the classical model is retrieved. The solution of proposed model remained convergent for any values of these parameters greater than or equal to zero. The values of the parameters in these simulations can be diverse; however the particular values have been selected from various sources already published in the literature; see, for example, [12–14, 53, 54].

6.3. Average Skin Friction Coefficient. The average skin friction coefficients for different parameters and for various

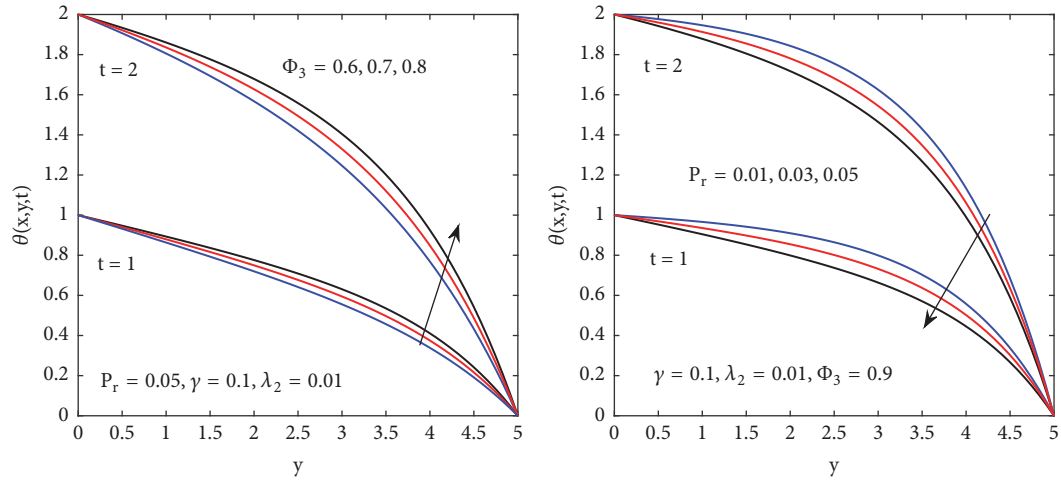

(a) Temperature distribution for Φ_3 (b) Temperature distribution for P_r

Figure 4

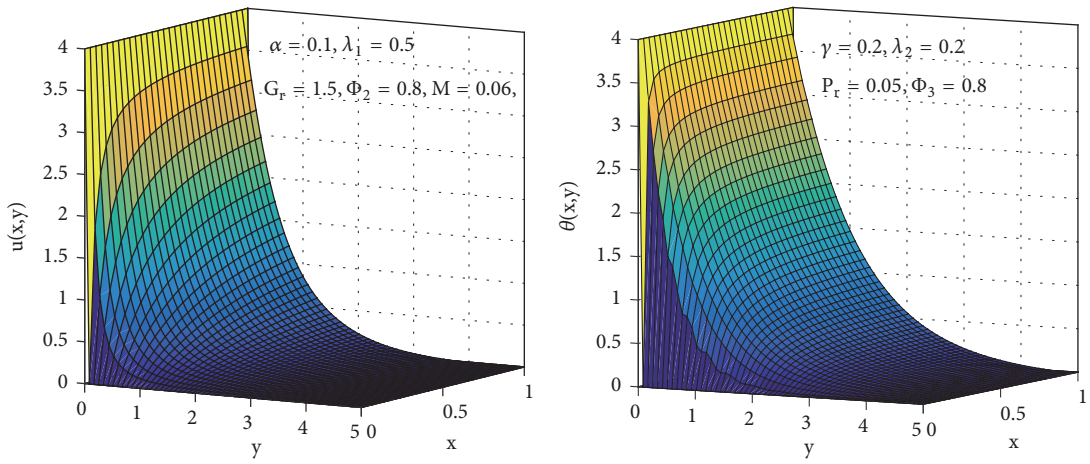

(a) Three-dimensional velocity distribution (b) Three-dimensional temperature distribution

Figure 5

values are shown in Table 1. Skin friction plays a vital role in predicting the behavior of flow in the vicinity of the boundary. Effects of different parameters on the skin friction coefficient can be used to show the cumulative trend of friction in the flow domain. The average skin friction coefficient decreases with the increase of fractional parameter α which shows that the momentum boundary layer thickness reduces along the plate or wall boundary. Similar trends have been observed for the increasing values of nanofluid parameter Φ_2 whereas opposite behavior has been observed while the values of magnetic field and relaxation parameter λ_1 augment; that is, the momentum boundary layer thickness extends.

6.4. Average Nusselt Number. Table 2 illustrates the influence of physical and fractional parameters on the average Nusselt number. Nusselt number is important for the calculation of thermal field variations along the wall or boundary. Realistic physical simulations can be executed if one takes into account the Nusselt number while calculating the thermal field. The numeric values of Nusselt number will be helpful to show the cumulative trend of temperature gradient in the flow domain. Average Nusselt number is comprehensive function of temperature gradient as shown in (48). For each increased value of γ, the average Nusselt number monotonically decreases which shows that less heat is transferred to the fluid from the plate. Similar behavior has been observed for the increasing values of the Prandtl number Pr, whereas increasing values of the thermal relaxation parameter λ_2 and the radiation parameter Φ_3 impose small increase on average Nusselt number which results in the greater heat exchange rate near the plate.

In Table 3, the comparison for different values of Prandtl number Pr has been presented with already published papers for the validation and accuracy of the numerical results. As it is the ratio of molecular diffusivity of momentum to the molecular diffusivity of heat, it shows the relative thickness

Table 3: Comparison of $-(\partial\theta/\partial y)|_{y=0}$ at $x = 1$, with $\alpha = 1$, $\gamma = 1$, $M = 0$, $\phi_3 = 0$, and $\lambda_1 = \lambda_2 = 0$.

Pr	Crepeau and clarksean [12]	Chamkha and khaled [13]	Chen [14]	present work
0.01	0.0805	0.0600	0.0806	0.0585
0.1	0.2302	0.2119	0.23014	0.2460
1	0.5671	0.5649	0.5671	0.6631
10	1.1690	1.1720	1.1693	1.1412
100	2.1910	2.1943	2.1913	2.1126

of the velocity boundary layer to the thermal boundary layer. The increase in the value of Pr basically describes dominance of momentum diffusivity over the thermal diffusivity. Crepeau and Clarksean [12], Chamkha and khaled [13], and Chen [14] compared the value of rate of change of heat at the surface $-\partial\theta/\partial y$ at $y = 0$ for various values of the Prandtl number Pr and other physical parameters. We have also compared the same for the similar values in order to validate our results.

7. Conclusion

In this paper we consider heat transfer in unsteady mixed convection flow of the Maxwell nanofluids on a horizontal moving plate along with vertically applied magnetic field and radiations. The fractional mathematical model is derived by introducing fractional time derivative into Maxwell constitutive equations. The governing equations are numerically solved by employing a newly developed finite difference method (FDM) combined with $L1$-algorithm [52]. The effects of fractional parameters α and γ along with other pertinent physical parameters on the velocity and temperature profiles have been discussed with the help of graphs for various values. The skin friction coefficient (Cf) and Nusselt number (Nu) have also been discussed for different values of physical parameters. In graphical results, the fractional parameter α increases the thickness of velocity and γ increases the thermal boundary layer. The variations of parameters λ_1, λ_2, P_r, M, Φ_2, and Φ_3 change the course of velocity and temperature profiles significantly as discussed with details in section 6. Fractional parameter α has main role on average skin friction coefficient and γ on average Nusselt number. It is concluded that the fractional parameters play a vital role to capture the memory of the viscoelastic fluid for different values of fractional values instead of only one fixed value of derivative, *i.e.*, $\alpha = \gamma = 1$. Momentum and thermal profiles are at lower level for all fractional values other than 1, which are quite helpful in predicting the realistic results.

Data Availability

No data is used in this study.

Conflicts of Interest

The authors declare that there are no conflicts of interest.

Authors' Contributions

All authors have read and reviewed the article and have the same contribution.

References

[1] J. C. Maxwell, "On the dynamical theory of gases," *Philosophical Transactions of the Royal Society London*, vol. A157, pp. 26–78, 1866.

[2] T. Hayat, M. I. Khan, M. Imtiaz, and A. Alsaedi, "Heat and mass transfer analysis in the stagnation region of maxwell fluid with chemical reaction over a stretched surface," *Journal of Thermal Science and Engineering Applications*, 2017.

[3] Z. Cao, J. Zhao, Z. Wang, F. Liu, and L. Zheng, "MHD flow and heat transfer of fractional Maxwell viscoelastic nanofluid over a moving plate," *Journal of Molecular Liquids*, vol. 222, pp. 1121–1127, 2016.

[4] Y. Liu and B. Guo, "Effects of second-order slip on the flow of a fractional Maxwell MHD fluid," *Journal of the Association of Arab Universities for Basic and Applied Sciences*, vol. 24, pp. 232–241, 2017.

[5] Y. Mahsud, N. A. Shah, and D. Vieru, "Influence of time-fractional derivatives on the boundary layer flow of Maxwell fluids," *Chinese Journal of Physics*, vol. 55, no. 4, pp. 1340–1351, 2017.

[6] M. Madhu, N. Kishan, and A. J. Chamkha, "Unsteady flow of a Maxwell nanofluid over a stretching surface in the presence of magnetohydrodynamic and thermal radiation effects," *Propulsion and Power Research*, vol. 6, no. 1, pp. 31–40, 2017.

[7] D. Vieru and A. Rauf, "Stokes flows of a Maxwell fluid with wall slip condition," *Canadian Journal of Physics*, vol. 89, no. 10, pp. 1061–1071, 2011.

[8] K.-L. Hsiao, "Combined electrical MHD heat transfer thermal extrusion system using Maxwell fluid with radiative and viscous dissipation effects," *Applied Thermal Engineering*, vol. 112, pp. 1281–1288, 2017.

[9] T. Hayat, T. Muhammad, S. A. Shehzad, and A. Alsaedi, "Three dimensional rotating flow of Maxwell nanofluid," *Journal of Molecular Liquids*, vol. 229, pp. 495–500, 2017.

[10] G. K. Ramesh, B. J. Gireesha, T. Hayat, and A. Alsaedi, "Stagnation point flow of Maxwell fluid towards a permeable surface in the presence of nanopar ticles," *Alexandria Engineering Journal*, vol. 55, no. 2, pp. 857–865, 2016.

[11] S. Mukhopadhyay, "Heat Transfer Analysis of the Unsteady Flow of a Maxwell Fluid over a Stretching Surface in the Presence of a Heat Source/Sink," *Chinese Physics Letters*, 2012.

[12] J. C. Crepeau and R. Clarksean, "Similarity solutions of natural convection with internal heat generation," *Journal of Heat Transfer*, vol. 119, no. 1, pp. 183–185, 1997.

[13] A. J. Chamkha and A.-R. A. Khaled, "Similarity solutions for hydromagnetic simultaneous heat and mass transfer by natural convection from an inclined plate with internal heat generation or absorption," *Heat and Mass Transfer*, vol. 37, no. 2-3, pp. 117–123, 2001.

[14] C.-H. Chen, "Combined heat and mass transfer in MHD free convection from a vertical surface with Ohmic heating and viscous dissipation," *International Journal of Engineering Science*, vol. 42, no. 7, pp. 699–713, 2004.

[15] S. U. S. Choi and J. A. Eastman, *Enhancing Thermal Conductivity of Fluids with Nanoparticles*, Argonne National Lab, Illinois, IL, USA, 1995.

[16] B. C. Prasannakumara, B. J. Gireesha, M. R. Krishnamurthy, and K. Ganesh Kumar, "MHD flow and nonlinear radiative heat transfer of Sisko nanofluid over a nonlinear stretching sheet," *Informatics in Medicine Unlocked*, vol. 9, pp. 123–132, 2017.

[17] K. G. Kumar, B. J. Gireesha, M. R. Krishnamurthy, and B. C. Prasannakumara, "Impact of Convective Condition on Marangoni Convection Flow and Heat Transfer in Casson Nanofluid with Uniform Heat Source Sink," *Journal of Nanofluids*, vol. 7, no. 1, pp. 108–114, 2018.

[18] M. Sheikholeslami and S. A. Shehzad, "Simulation of water based nanofluid convective flow inside a porous enclosure via non-equilibrium model," *International Journal of Heat and Mass Transfer*, vol. 120, pp. 1200–1212, 2018.

[19] M. Turkyilmazoglu and I. Pop, "Heat and mass transfer of unsteady natural convection flow of some nanofluids past a vertical infinite flat plate with radiation effect," *International Journal of Heat and Mass Transfer*, vol. 59, no. 1, pp. 167–171, 2013.

[20] M. Sheikholeslami and H. B. Rokni, "Numerical simulation for impact of Coulomb force on nanofluid heat transfer in a porous enclosure in presence of thermal radiation," *International Journal of Heat and Mass Transfer*, vol. 118, pp. 823–831, 2018.

[21] K. G. Kumar, G. K. Ramesh, B. J. Gireesha, and R. S. R. Gorla, "Characteristics of Joule heating and viscous dissipation on three-dimensional flow of Oldroyd B nanofluid with thermal radiation," *Alexandria Engineering Journal*, 2017.

[22] M. Usman, R. U. Haq, M. Hamid, and W. Wang, "Least square study of heat transfer of water based Cu and Ag nanoparticles along a converging/diverging channel," *Journal of Molecular Liquids*, vol. 249, pp. 856–867, 2018.

[23] M. S. Anwar and A. Rasheed, "Heat transfer at microscopic level in a MHD fractional inertial flow confined between non-isothermal boundaries," *European Physical Journal Plus*, vol. 132, pp. 305–322, 2017.

[24] M. Sheikholeslami, M. Darzi, and M. K. Sadoughi, "Heat transfer improvement and pressure drop during condensation of refrigerant-based nanofluid; an experimental procedure," *International Journal of Heat and Mass Transfer*, vol. 122, pp. 643–650, 2018.

[25] K. Bhattacharyya, S. Mukhopadhyay, G. C. Layek, and I. Pop, "Effects of thermal radiation on micropolar fluid flow and heat transfer over a porous shrinking sheet," *International Journal of Heat and Mass Transfer*, vol. 55, no. 11-12, pp. 2945–2952, 2012.

[26] K. Bhattacharyya, "MHD stagnation-point flow of casson fluid and heat transfer over a stretching sheet with thermal radiation," *Journal of Thermodynamics*, vol. 2013, Article ID 169674, 9 pages, 2013.

[27] T. Hayat, M. Waqas, S. A. Shehzad, and A. Alsaedi, "Mixed convection radiative flow of maxwell fluid near a stagnation point with convective condition," *Journal of Mechanics*, vol. 29, no. 3, pp. 403–409, 2012.

[28] Y. Zakariya, Y. Afolabi, R. Nuruddeen, and I. Sarumi, "Analytical solutions to fractional fluid flow and oscillatory process models," *Fractal and Fractional*, vol. 2, no. 2, p. 18, 2018.

[29] Y. Zhang, H. Zhao, F. Liu, and Y. Bai, "Analytical and numerical solutions of the unsteady 2D flow of MHD fractional Maxwell fluid induced by variable pressure gradient," *Computers & Mathematics with Applications. An International Journal*, vol. 75, no. 3, pp. 965–980, 2018.

[30] N. Cusimano and L. Gerardo-Giorda, "A space-fractional monodomain model for cardiac electrophysiology combining anisotropy and heterogeneity on realistic geometries," *Journal of Computational Physics*, vol. 362, pp. 409–424, 2018.

[31] J. M. Cruz-Duarte, J. Rosales-Garcia, C. R. Correa-Cely, A. Garcia-Perez, and J. G. Avina-Cervantes, "A closed form expression for the Gaussian-based Caputo-Fabrizio fractional derivative for signal processing applications," *Communications in Nonlinear Science and Numerical Simulation*, vol. 61, pp. 138–148, 2018.

[32] K. Assaleh and W. M. Ahmad, "Modeling of speech signals using fractional calculus," in *Proceedings of the 2007 9th International Symposium on Signal Processing and Its Applications, ISSPA*, February 2007.

[33] J. F. Douglas, "Some applications of fractional calculus to polymer science," in *Advances in Chemical Physics*, vol. 102, John Wiley and Sons, Inc, 1997.

[34] Z. E. A. Fellah, C. Depollier, and M. Fellah, "Application of fractional calculus to the sound waves propagation in rigid porous materials: Validation via ultrasonic measurements," *Acta Acustica united with Acustica*, vol. 88, no. 1, pp. 34–39, 2002.

[35] G. A. Losa, D. Merlini, T. F. Nonnenmacher, and E. R. Weibel, *Fractals in Biology and Medicine*, Birkhauser Verlag, 2005.

[36] L. Lu and X. Yu, "The fractional dynamics of quantum systems," *Annals of Physics*, vol. 392, pp. 260–271, 2018.

[37] A. Beltempo, M. Zingales, O. S. Bursi, and L. Deseri, "A fractional-order model for aging materials: An application to concrete," *International Journal of Solids and Structures*, vol. 138, pp. 13–23, 2018.

[38] A. B. Salati, M. Shamsi, and D. F. M. Torres, "Direct transcription methods based on fractional integral approximation formulas for solving nonlinear fractional optimal control problems," *Communications in Nonlinear Science and Numerical Simulation*, vol. 67, pp. 334–350, 2019.

[39] C. Fetecau, D. Vieru, and W. A. Azhar, "Natural convection flow of fractional nanofluids over an isothermal vertical plate with thermal radiation," *Applied Sciences (Switzerland)*, vol. 7, no. 3, 2017.

[40] N. Ali Shah, D. Vieru, and C. Fetecau, "Effects of the fractional order and magnetic field on the blood flow in cylindrical domains," *Journal of Magnetism and Magnetic Materials*, vol. 409, pp. 10–19, 2016.

[41] M. S. Anwar and A. Rasheed, "Simulations of a fractional rate type nanofluid flow with non-integer Caputo time derivatives," *Computers & Mathematics with Applications. An International Journal*, vol. 74, no. 10, pp. 2485–2502, 2017.

[42] M. A. Asjad, M. B. Riaz, N. A. Shah, and A. A. Zafar, "Boundary layer flow of MHD generalized Maxwell fluid over an exponentially accelerated infinite vertical surface with slip and Newtonian heating at the boundary," *Results in Physics*, vol. 8, pp. 1061–1067, 2018.

[43] M. I. Asjad, N. A. Shah, M. Aleem, and I. Khan, "MHD Time Fractional Natural Convection Flow of a Viscous Fluid through Porous Medium," *Journal of Porous Materials*, 2018.

[44] C. Fetecau, N. Ali Shah, and D. Vieru, "General Solutions for Hydromagnetic Free Convection Flow over an Infinite Plate with Newtonian Heating, Mass Diffusion and Chemical Reaction," *Communications in Theoretical Physics*, vol. 68, no. 6, pp. 768–782, 2017.

[45] Q. Al-Mdallal, K. A. Abro, and I. Khan, "Analytical Solutions of Fractional Walter's B Fluid with Applications," *Complexity*, vol. 2018, Article ID 8131329, 10 pages, 2018.

[46] C. Friedrich, "Relaxation and retardation functions of the Maxwell model with fractional derivatives," *Rheologica Acta*, vol. 30, no. 2, pp. 151–158, 1991.

[47] Z.-Q. Chen, "Time fractional equations and probabilistic representation," *Chaos, Solitons & Fractals*, vol. 102, pp. 168–174, 2017.

[48] C. Cattaneo, "Sur une forme de l'équation de la chaleur éliminant le paradoxe d'une propagation instantanée," *Comptes rendus de l'Académie des Sciences*, vol. 247, pp. 431–433, 1958.

[49] T. Hayat, S. Asad, and A. Alsaedi, "Flow of variable thermal conductivity fluid due to inclined stretching cylinder with viscous dissipation and thermal radiation," *Applied Mathematics and Mechanics-English Edition*, vol. 35, no. 6, pp. 717–728, 2014.

[50] H. F. Oztop and E. Abu-Nada, "Numerical study of natural convection in partially heated rectangular enclosures filled with nanofluids," *International Journal of Heat and Fluid Flow*, vol. 29, no. 5, pp. 1326–1336, 2008.

[51] V. E. Lynch, B. A. Carreras, D. del-Castillo-Negrete, K. M. Ferreira-Mejias, and H. R. Hicks, "Numerical methods for the solution of partial differential equations of fractional order," *Journal of Computational Physics*, vol. 192, no. 2, pp. 406–421, 2003.

[52] F. Liu, P. Zhuang, V. Anh, I. Turner, and K. Burrage, "Stability and convergence of the difference methods for the space-time fractional advection-diffusion equation," *Applied Mathematics and Computation*, vol. 191, no. 1, pp. 12–20, 2007.

[53] J. Zhao, L. Zheng, X. Zhang, and F. Liu, "Unsteady natural convection boundary layer heat transfer of fractional Maxwell viscoelastic fluid over a vertical plate," *International Journal of Heat and Mass Transfer*, vol. 97, pp. 760–766, 2016.

[54] P. Ganesan and G. Palani, "Finite difference analysis of unsteady natural convection MHD flow past an inclined plate with variable surface heat and mass flux," *International Journal of Heat and Mass Transfer*, vol. 47, no. 19-20, pp. 4449–4457, 2004.